



# Immobilisation on mesoporous silica and solvent rinsing improve the transesterification abilities of feruloyl esterases from *Myceliophthora thermophila*



Silvia Hüttner<sup>a</sup>, Milene Zezzi Do Valle Gomes<sup>b</sup>, Laura Iancu<sup>c</sup>, Anders Palmqvist<sup>b</sup>, Lisbeth Olsson<sup>a,\*</sup>

<sup>a</sup> Department of Biology and Biological Engineering, Division of Industrial Biotechnology, Chalmers University of Technology, SE-412 96 Gothenburg, Sweden

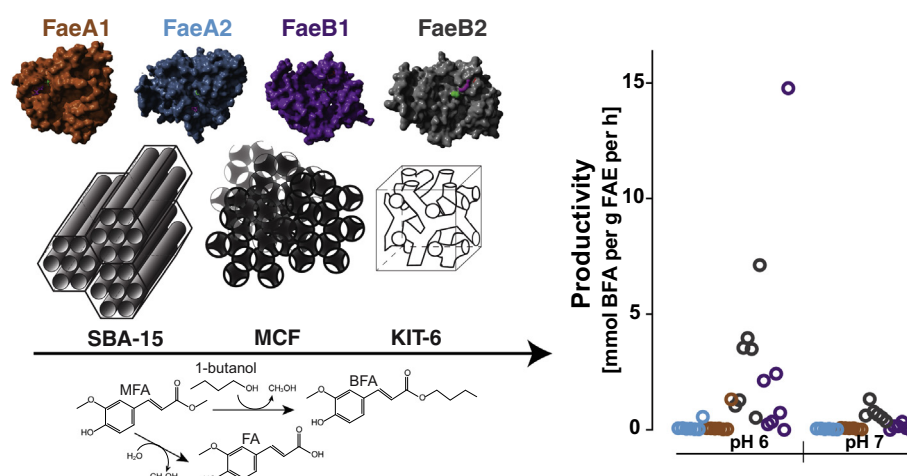
<sup>b</sup> Department of Chemistry and Chemical Engineering, Division of Applied Chemistry, Chalmers University of Technology, SE-412 96 Gothenburg, Sweden

<sup>c</sup> DuPont Industrial Biosciences, Nieuwe Kanaal 7S, 6709 PA Wageningen, The Netherlands

## HIGHLIGHTS

- Four FAEs from *M. thermophila* C1 were immobilised on mesoporous silica.
- Size-selective immobilisation of proteins was observed.
- Immobilised enzymes were used for transesterification reactions in solvents.
- Enzymes could be reused in nine reaction cycles with less than 10% activity loss.
- Solvent rinsing improved transesterification yield compared to conventional drying.

## GRAPHICAL ABSTRACT



## ARTICLE INFO

### Article history:

Received 20 February 2017  
Received in revised form 25 April 2017  
Accepted 26 April 2017  
Available online 29 April 2017

### Keywords:

SBA-15  
Butyl ferulate  
Biocatalysis  
Esterification  
Enzyme immobilisation

## ABSTRACT

The immobilisation of four feruloyl esterases (FAEs) (FaeA1, FaeA2, FaeB1, FaeB2) from the thermophilic fungus *Myceliophthora thermophila* C1 was studied and optimised via physical adsorption onto various mesoporous silica particles with pore diameters varying from 6.6 nm to 10.9 nm. Using crude enzyme preparations, enrichment of immobilised FAEs was observed, depending on pore diameter and protein size. The immobilised enzymes were successfully used for the synthesis of butyl ferulate through transesterification of methyl ferulate with 1-butanol. Although the highest butyl ferulate yields were obtained with free enzyme, the synthesis-to-hydrolysis ratio was higher when using immobilised enzymes. Over 90% of the initial activity was observed in a reusability experiment after nine reaction cycles, each lasting 24 h. Rinsing with solvent to remove water from the immobilised enzymes further improved their activity. This study demonstrates the suitability of immobilised crude enzyme preparations in the development of biocatalysts for esterification reactions.

© 2017 The Authors. Published by Elsevier Ltd. This is an open access article under the CC BY-NC-ND license (<http://creativecommons.org/licenses/by-nc-nd/4.0/>).

\* Corresponding author.

E-mail addresses: [huttner@chalmers.se](mailto:huttner@chalmers.se) (S. Hüttner), [milene@chalmers.se](mailto:milene@chalmers.se) (M. Zezzi Do Valle Gomes), [laura.iancu@dupont.com](mailto:laura.iancu@dupont.com) (L. Iancu), [anders.palmqvist@chalmers.se](mailto:anders.palmqvist@chalmers.se) (A. Palmqvist), [lisbeth.olsson@chalmers.se](mailto:lisbeth.olsson@chalmers.se) (L. Olsson).

## 1. Introduction

Ferulic acid (FA) and other hydroxycinnamic acids are naturally occurring, bioactive phenolic compounds that have been shown to have antifungal, antibacterial, anti-inflammatory, antiviral and UV absorptive properties, as well as potential positive effects on age-related and neurodegenerative diseases (Tan and Shahidi, 2011; Barone et al., 2009; Tawat et al., 1996). Feruloyl esterases (FAEs, E.C. 3.1.1.73; Crepin et al., 2004; Gopalan et al., 2015; Kroon et al., 1999) can be used to carry out esterification reactions between FA and alcohol or sugar groups (Giuliani et al., 2001; Matsuo et al., 2008; Thörn et al., 2011; Vafiadi et al., 2009). The resulting change in hydrophobicity/hydrophilicity of the original compounds broadens their applicability as antioxidants in the cosmetics, food and pharmaceutical industries (Antonopoulou et al., 2016; Faulds, 2010). To minimise or avoid the hydrolytic reaction carried out by the enzymes in nature, (trans)esterification reactions must take place in organic solvents with low water content. This suppresses hydrolytic activity, and can also increase the solubility of hydrophobic substances, shifting the thermodynamic equilibrium towards synthesis rather than hydrolysis (Carrea and Riva, 2000). However, it also constitutes an unfavourable environment for most enzymes (Hudson et al., 2005; Serdakowski and Dordick, 2008; Soares et al., 2003; Yang et al., 2004). One strategy widely used to counteract the deleterious effects of organic solvents in industrial applications, is enzyme immobilisation (Eş et al., 2015; Stepankova et al., 2013). The increased stability of immobilised biocatalysts is attributed to the stabilisation of the active conformation and the prevention of unfolding or malformation. Another advantage of enzyme immobilisation is the efficient and relatively easy recovery of enzymes from the reaction media, separation from the product, and the ability to employ a continuous process, thus reducing the amount of enzyme required, and thus the production cost. Immobilisation can lead to a reduction in enzymatic activity; a disadvantage which is, however, counterbalanced by the ability to use the same batch of enzyme for many production cycles (Essa et al., 2007; Singh et al., 2013).

Mesoporous silica (MPS) is one of the most widely used and studied support materials for enzyme adsorption (Magner, 2013; Moelans et al., 2005; Zhou and Hartmann, 2012), a simple and inexpensive method of immobilisation that does not involve covalent bonds between the enzyme and the support material (Brady and Jordaan, 2009; Sheldon and van Pelt, 2013). MPS has an ordered pore structure, a large surface area, high stability and a narrow pore distribution. The parameters and kinetics governing adsorption depend on both the biocatalyst and the specific support used (Cao, 2005), and attempts have been made to correlate immobilisation conditions with the three-dimensional structure, size and surface potential of the enzyme of interest (Essa et al., 2007; Thörn et al., 2013).

The aim of the present study was to optimise the production of butyl ferulate (BFA) by transesterification reactions with immobilised enzymes. BFA has been shown to have radical-scavenging and antioxidant activities (Kikuzaki et al., 2002) and is more lipophilic than ferulic acid, and thus attractive for use in cosmetics and pharmaceuticals. Four FAEs from crude fungal culture filtrates of the thermophilic fungus *Myceliophthora thermophila* C1 (Kühnel et al., 2012; Visser et al., 2011) were compared upon adsorption onto MPS with six different pore sizes and geometries, with the goal of maximising the BFA productivity and product selectivity. The effects of solvent-rinsing and reuse of enzyme-loaded MPS on transesterification activity were also investigated.

## 2. Materials and methods

### 2.1. Chemicals

HPLC grade methyl ferulate (MFA) and FA were purchased from Apin Chemicals Ltd., UK. BFA was kindly provided as a gift by Evangelos Topakas, National Technical University of Athens, Greece. All other chemicals were purchased from Sigma-Aldrich.

### 2.2. Enzymes

The *M. thermophila* C1 genes encoding the FAEs FaeA1, FaeA2, FaeB1 and FaeB2 were expressed individually in designated C1 hosts with low cellulase production background (Kühnel et al., 2012; Visser et al., 2011). The biomass-free fermentation broth was concentrated and dialysed, and the resulting crude FAE extract was freeze-dried until use. The total protein samples (i.e., crude culture filtrates) are denoted C1FaeA1, C1FaeA2, C1FaeB1 and C1FaeB2, whereas the specific FAE enzymes are denoted FaeA1, FaeA2, FaeB1 and FaeB2. The primary amino acid sequences can be found under the Genbank accessions JF826027.1 (FaeA1), JF826028.1 (FaeA2), KX889209 (FaeB1) and JF826029.1 (FaeB2). Homology modelling was performed with the online-tool Phyre2 (<http://www.sbg.bio.ic.ac.uk/phyre2>) (Kelly et al., 2015), and visualisation with YASARA (<http://www.yasara.org/>) (Krieger and Vriend, 2014).

### 2.3. Synthesis of mesoporous silica

MPS particles with three different pore morphologies were synthesised: SBA-15, mesostructured cellular foam (MCF) and KIT-6. Tetraethyl orthosilicate (TEOS) was used as the silica precursor and Pluronic P123 ( $\text{EO}_{20}\text{PO}_{70}\text{EO}_{20}$ ,  $M_w = 5800$ ) as the structure-directing agent in all syntheses. A procedure described previously (Gustafsson et al., 2012) was adapted for the synthesis of SBA-15 particles with pore sizes of 7.8, 8.7, 10.1 and 10.2 nm. MCF was synthesised according to the method developed by Schmidt-Winkel et al. (2000), using trimethylbenzene (TMB) as a swelling agent to obtain a pore size of 26.5 nm and a window size of 10.9 nm. KIT-6 with 6.6 nm pore size was prepared following the procedure described by Kleitz et al. (2003). A more detailed description of the synthesis procedures can be found in Appendix A. The MPS particles were characterised by nitrogen sorption analysis using a Micrometrics ASAP 2010 instrument. Prior to the adsorption measurements, the samples were outgassed at 180 °C for at least 6 h. The surface area was determined using the BET (Brunauer-Emmett-Teller) method (Brunauer et al., 1938). The pore size distributions of the SBA-15 and the KIT-6 particles were determined using the BJH (Barrett-Joyner-Halenda) method (Barrett et al., 1951), whereas for the MCF the simplified BdB-FHH method (Lukens et al., 1999) was used to calculate the pore size (using the adsorption isotherm) and the window size (using the desorption isotherm).

### 2.4. Immobilisation of proteins

The MPS particles were prepared for immobilisation by washing five times with immobilisation buffer (0.1 M citrate phosphate pH 3–7, 0.1 M Tris-HCl pH 7–9). Protein solutions were then added to the washed MPS particles and incubated on a mixing rotator at 4 °C for 18 h. After incubation, the protein-loaded MPS particles were washed three times with immobilisation buffer to remove unbound protein. The protein-loaded MPS particles were either dried (in a SpeedVac vacuum concentrator at room temperature

for 1 h) or rinsed with an organic solvent. Dried or solvent-rinsed protein-loaded MPS was stored at 4 °C until use.

### 2.5. Solvent-rinsed enzyme preparations

Solvent-rinsed enzyme preparations (PREPs) were prepared as described previously (Partridge et al., 1998). Briefly, after immobilisation, washed protein-loaded MPS was rinsed five times with 1-butanol, 1-propanol or ethanol, with or without added buffer, and stored until use at 4 °C in the same solvent as was used for rinsing. To determine the amount of buffer to be added to the PREPs to reach a certain water activity ( $a_w$ ), the Wilson equation was used (Vulfson and Halling, 2001). Equations used can be found in Appendix A. Before use in transesterification reactions, the PREPs were rinsed three times with the reaction solvent system. In order to study the reusability of the immobilised enzymes, the PREPs were washed twice between each cycle with 1-butanol-buffer (92.5:7.5, v/v) before starting a new reaction.

### 2.6. Measurement of protein concentration and hydrolysis reaction product

The amount of immobilised protein, or protein loading ( $\text{mg}_{\text{protein}} \text{mg}_{\text{MPS}}^{-1}$ ), was determined indirectly by measuring the protein concentration in the solution before and after immobilisation, using the BCA method (Pierce BCA protein assay kit, Thermo Fisher Scientific). To visualise size-dependent protein immobilisation over time, proteins were separated by SDS-PAGE on stain-free TGX gels and visualised on a GelDoc EZ system (both Bio-Rad). To determine the FAE loading ( $\text{mg}_{\text{FAE}} \text{mg}_{\text{MPS}}^{-1}$ ) on the MPS, the amount of immobilised FAE was calculated as the difference between the total amount of active enzyme in the original sample (known from densitometric analysis; Table 1) and the percentage of actual immobilised enzymes, which was determined by measuring the hydrolytic FAE activity in the supernatant before and after immobilisation. The hydrolytic FAE activity was determined by hydrolysis of MFA, as described previously (Yue et al., 2009). One unit of enzyme activity (1U) was defined as the amount of enzyme releasing 1  $\mu\text{mol}$  of FA per minute per mL.

### 2.7. Transesterification reactions and product analysis

The transesterification reactions (Supplementary Fig. S1a) were carried out using 30 mM MFA as the acceptor. Solvent and alcohol donor 1-butanol, and buffer (0.1 M citrate phosphate buffer, pH 6.5) were added in a ratio of 92.5:7.5 (v/v), which has previously been determined to be suitable for another FAE (Thörn et al., 2011). Enzyme was added either as free enzyme in the buffer fraction (75  $\mu\text{L}$  of a 0.4  $\text{mg mL}^{-1}$  protein solution in 1000  $\mu\text{L}$  reaction volume), or as dried or solvent-rinsed immobilised enzyme on MPS (5 mg enzyme-loaded MPS per mL of the 1-butanol-buffer mixture). Reactions with volumes of 250–1000  $\mu\text{L}$  were carried

out in 1.5 mL Eppendorf tubes sealed with Parafilm, on a thermoshaker at 30 °C and 1400 rpm. The detection and quantification of FA, MFA and BFA were carried out as described previously (Thörn et al., 2011) by HPLC (Dionex Ultimate 3000) using a Kinetex 2.6  $\mu\text{m}$  100  $\times$  4.6 mm C18 column (Phenomenex) with an isocratic elution profile of methanol and 3.33% acetic acid (7:3, v/v) (Supplementary Fig. S1b). Product selectivity was defined as the BFA:FA molar ratio, i.e., the amount of BFA produced divided by the amount of FA produced at a specific time. A BFA:FA ratio greater than 1 indicates that synthesis dominates over hydrolysis.

## 3. Results and discussion

### 3.1. Immobilisation of feruloyl esterases from *M. thermophila* on MPS

Proteins in crude culture filtrates of *M. thermophila* C1 fermentations containing different amounts of the active FAE enzymes FaeA1, FaeA2, FaeB1 or FaeB2 were immobilised on SBA-15 with a pore size of 10.1 nm (information about the samples is presented in Table 1). Since adsorption of proteins onto a silica support is mostly mediated by electrostatic interactions, and to a lesser degree by hydrophobic interactions and van der Waals forces, the maximum loading is achieved at maximum charge difference between the support and the protein surface. The theoretical pI of SBA-15 has been determined to be 3.8 (Essa et al., 2007), meaning that at a pH above 3.8 the overall charge of the silica is negative. The highest protein adsorption for the C1 samples was observed at pH values <5, indicating that the majority of the proteins in the crude culture filtrates carry a surface net positive charge at pH values below 5. Adsorption was studied over time to determine the time required for maximum immobilisation. The adsorption of total protein was very rapid in the first ten minutes, and reached equilibrium after approximately one to three hours (Fig. 1a), in agreement with previous observations (Thörn et al., 2011). The effect of pH could be seen over the whole course of the experiment; adsorption was more rapid and more efficient at lower pH values than at higher pH values. For example, for sample C1FaeB1, 77% of the total protein was immobilised at pH 5, 60% at pH 6, but only 17% at pH 7 (Fig. 1a,c).

Residual enzyme activity in the liquid fraction was determined over the course of immobilisation to indirectly determine the amount of FAE enzymes immobilised. The immobilisation of FAE activity was rapid during the first hour and reached an equilibrium after about three hours (Fig. 1b). This is in agreement with the total protein adsorption shown in Fig. 1a. Generally, more FAE activity was immobilised at lower pH values (pH 5) than at higher pH values (pH 7). This is in accordance with the calculated pI values of the four enzymes, all of which were higher than the pI of SBA-15 (Table 1). Interestingly, a higher percentage of enzyme activity than percentage of total protein was removed from the

**Table 1**  
Properties of the four FAEs studied in the *M. thermophila* C1 culture filtrates.

Sample	FAE	FAE content ( $\text{mg}_{\text{FAE}} \text{mg}_{\text{protein}}^{-1}$ ) <sup>1</sup>	pI of FAE <sup>2</sup>	Molecular weight of FAE (kDa) <sup>3</sup>	Estimated size of FAE (nm) <sup>4</sup>
C1FaeA1	FaeA1	0.337	6.17	30	5.5 $\times$ 4.6 $\times$ 4.2
C1FaeA2	FaeA2	0.150	5.47	39	5.3 $\times$ 4.9 $\times$ 3.2
C1FaeB1	FaeB1	0.500	6.53	30	7.1 $\times$ 5.1 $\times$ 4.0
C1FaeB2	FaeB2	0.100	4.19	35	6.3 $\times$ 4.7 $\times$ 3.7

<sup>1</sup> Estimated by densitometric analysis on SDS-PAGE gels.

<sup>2</sup> Calculated with Snappgene 3.0.3.

<sup>3</sup> Estimated from SDS-PAGE data.

<sup>4</sup> Determined from homology modelling.

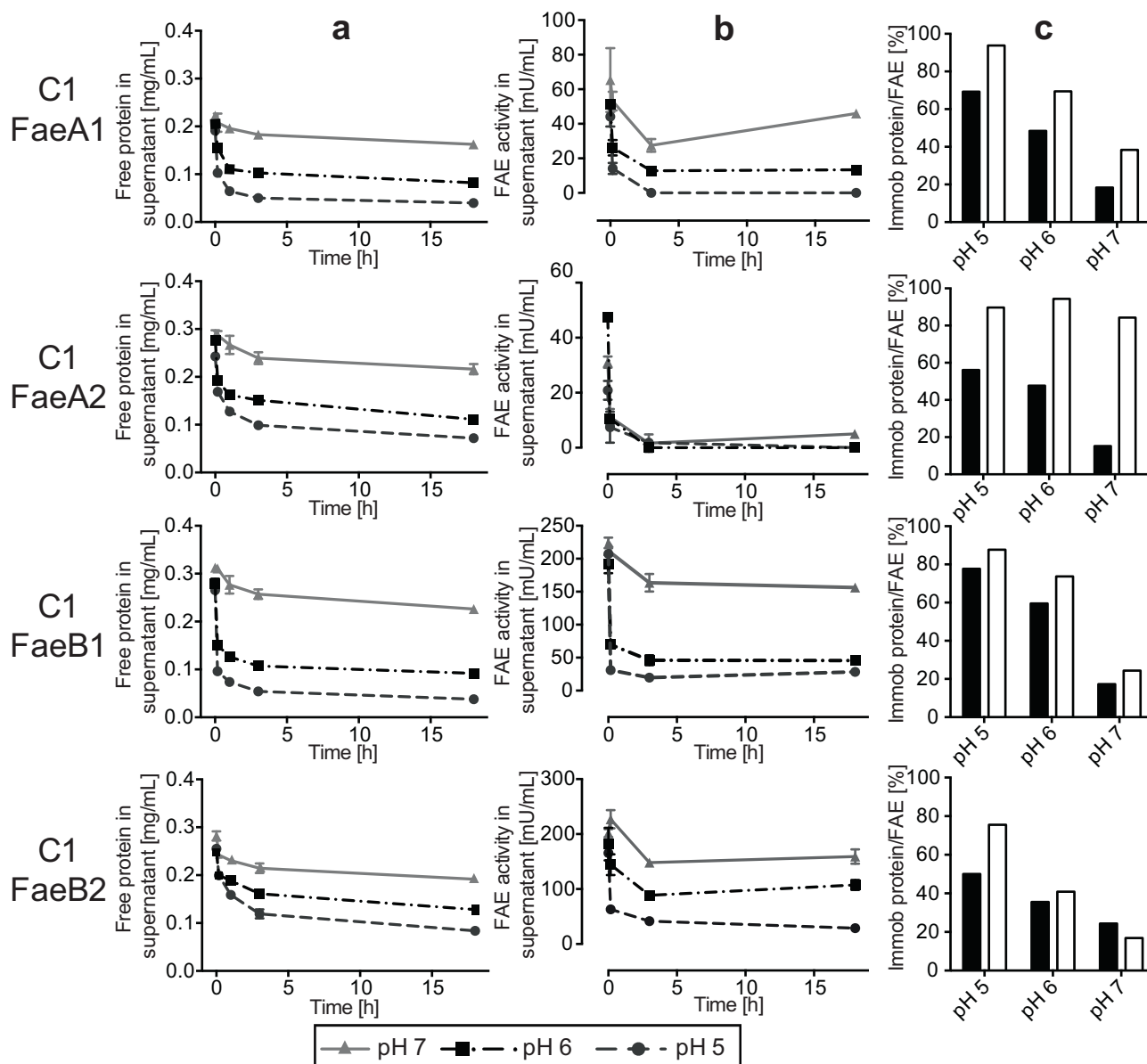


**Fig. 1.** Protein and enzyme adsorption onto SBA-15 with 10.1 nm pores as a function of time at three different pH values, visualised by depletion of protein concentration (a) or enzyme activity (b) in the supernatant. Total proteins from samples C1FaeA1, C1FaeA2, C1FaeB1 and C1FaeB2 were allowed to adsorb at 4 °C over the course of 18 h. The average of three independent experiments is shown, and the error bars indicate the standard deviation. (c) Percentage of immobilised protein (black shaded bars) and immobilised FAE (white bars) after 18 h.

**Table 2**  
Properties of mesoporous silica (MPS) substrates studied, determined by nitrogen adsorption analysis.

MPS	Pore size (nm)	BET surface area (m <sup>2</sup> g <sup>-1</sup> )	Pore volume (cm <sup>3</sup> g <sup>-1</sup> )
SBA-15 7.8 nm	7.8	703	1.09
SBA-15 8.7 nm	8.7	546	1.25
SBA-15 10.1 nm	10.1	415	1.11
SBA-15 10.2 nm	10.2	467	1.28
MCF	26.5, 10.9 <sup>1</sup>	523	1.94
KIT-6	6.6	624	0.98

<sup>1</sup> Window size (nm).

supernatant in almost all samples tested at all pH values (Fig. 1c). This suggests that FAEs are more efficiently immobilised than other proteins in the samples.

### 3.2. Size-selective immobilisation of crude enzymes

To evaluate how immobilisation influences the enzymatic activity and stability of the biocatalysts, and how pore size and pore structure affect those parameters, MPS with different geometries and dimensions were included in the study (Table 2). SBA-15 has a hexagonal, rod-shaped structure with round, straight pores of defined sizes, MCF has a foam-like structure consisting of pores connected via 'windows', while KIT-6 has a cage-like structure. These differences in geometry and pore size lead to different surface areas and pore volumes (Table 2).

The size of the protein of interest is arguably the most important consideration when designing the ideal support material for immobilisation. The three-dimensional structures of the four FAEs included in this study have not yet been experimentally determined, but their sizes were estimated using homology modelling

(Table 1, Supplementary Fig. S2). Modelling showed that FaeA1, FaeA2, FaeB1 and FaeB2 have similar dimensions, of about  $7 \times 5 \times 4$  nm, and they should thus theoretically fit into the pores of all the MPS materials investigated (Table 2), with the possible exception of KIT-6 (pore size 6.6 nm).

After adsorption onto MPS, proteins in the size range of about 25–50 kDa (which corresponds to a globular protein of 4–5 nm in diameter) were much more depleted from the supernatant than larger proteins, as can be seen by the lighter staining pattern on the SDS-PAGE gel (Fig. 2a). Thus, a certain degree of enrichment of the FAEs and exclusion of background proteins could be achieved through immobilisation, as suggested by the results given above, where the percentage of immobilised FAE was higher than the percentage of immobilised protein (expressed as the % of the total) (Fig. 1c). The rapid progression of protein adsorption (Fig. 1a) was also reflected in the SDS-PAGE results, as the prominent FaeB1-specific band at about 30 kDa is significantly fainter after only 10 min (Fig. 2b).

A correlation was found between pore size and the depletion of FAE in the supernatant; the larger the pores, the greater the reduction in FAE in the supernatant, i.e. the greater the adsorption into the pores (Fig. 2c). However, with increasing pore size, more of the larger proteins were immobilised.

More total protein was adsorbed per gram of MPS at pH 6 than at pH 7 for all enzymes and MPSs (Table 3). The interaction of FAEs with the silica was also expected to be stronger at pH 6 than at pH 7, since at the lower pH value a larger area of the protein surface is positively charged, and will therefore be attracted to the negatively charged surface of the support material. This was confirmed by simulating the surface charge distribution of the enzymes at different pH values using homology modelling (Supplementary Fig. S3).

A clear relation was observed of higher protein and FAE immobilisation on material with larger pores. Surprisingly, however, the material with the largest pores, MCF, showed FAE loadings similar to or lower than that on the material with the smallest pore diameter, KIT-6, for all samples except C1FaeB2. This suggests that the geometry of the MPS material also plays a role in immobilisation efficiency, since it is the only parameter distinguishing the MPS materials from each other, besides pore diameter. The straighter pores of SBA-15 might be more accommodating to the proteins than the foam-like structure of MCF, or they might be less prone to clogging, since there are fewer bends where proteins could accumulate.

Taking pore size, pore surface area and pore volume into consideration, we saw that the major factor limiting protein immobilisation on the MPS materials studied was the pore size. SBA-15 with a pore diameter of 7.8 nm had the highest surface area of the materials investigated (1.5 times higher than SBA-15 with 10.2 nm pores (Table 2)), but could only accommodate a comparatively small amount of enzymes (Supplementary Figs. S4–S7). If pore volume were the limiting factor, the material with the highest pore volume, MCF, should be able to accommodate the most protein. However, the lowest amount of enzyme per  $\text{cm}^3$  MPS adsorbed was on MCF. This supports the theory that proteins can enter the pore spaces of SBA-15 more easily than of those of MCF. This stands, however, in contrast to a previous study where higher loading of horseradish peroxidase was found on MCF compared to SBA-15 (Chouyyok et al., 2009). The mechanism of protein diffusion into the pores of mesoporous silica of different geometries needs to be the subject of future investigations.

### 3.3. Transesterification with immobilised enzymes

Previous studies have shown that the enzyme activity after immobilisation is dependent on the immobilisation pH (Thörn et al., 2013). We also observed that enzymes immobilised at pH values  $<5$  did not show any activity, even when the subsequent reaction was run at neutral pH (data not shown). Thus, the conditions under which maximal enzyme loading was achieved were not optimal for maximal enzyme activity. In addition, pore size and curvature of the MPS material can also influence enzymatic activity, possibly through mechanisms such as molecular crowding and interactions with the surface that stabilise the active conformation of the enzyme (Dunker and Fernández, 2007; Lei et al., 2007; Thörn et al., 2011; Sang and Coppens, 2011). To investigate the influence of immobilisation pH as well as MPS geometry on synthetic FAE activity, immobilised enzymes were investigated in a transesterification model reaction. The BFA productivities when using the total protein samples C1FaeB1 and C1FaeB2 were almost two orders of magnitude higher than those obtained with C1FaeA1 and C1FaeA2 (Fig. 3), indicating that the enzymes FaeB1 and FaeB2 are better suited to the transesterification reaction. The best results were achieved with C1FaeB1 immobilised at pH 6 on SBA-15 with pores of 10.1 nm or 10.2 nm, or on MCF, resulting in productivities of 3.55, 3.97 and 3.50  $\text{mmol BFA g}^{-1} \text{h}^{-1}$ , respectively. The productivity varied when using C1FaeB2 for transesterification;

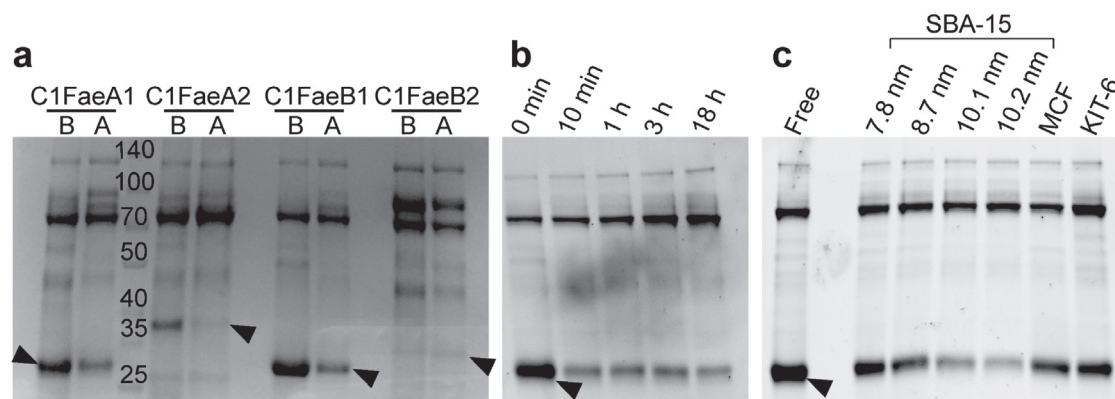


**Fig. 2.** Results of SDS-PAGE of supernatants from samples C1FaeA1, C1FaeA2, C1FaeB1 and C1FaeB2 before and after immobilisation. Fainter bands or missing bands are assumed to indicate immobilisation of the protein after adsorption. Black arrow heads indicate the specific bands of the FAEs FaeA1, FaeA2, FaeB1 and FaeB2. All samples were immobilised on MPS at pH 6 for 18 h, unless otherwise indicated. (a) Total protein samples before (B) and after (A) adsorption on SBA-15 with 10.1 nm pores. (b) Adsorption of C1FaeB1 on SBA-15 with 10.1 nm pores at different time points. (c) Adsorption of C1FaeB1 on the six different MPS substrates, as well as protein sample before adsorption (Free).

**Table 3**  
Amounts of protein and FAE immobilised per g MPS at pH 6 and pH 7.

		MPS	Protein (mg g <sup>-1</sup> MPS)	FAE (mg g <sup>-1</sup> MPS)			MPS	Protein (mg g <sup>-1</sup> MPS)	FAE (mg g <sup>-1</sup> MPS)
C1FaeA1	pH 6	7.8 nm	26.6 ± 0.7	13.1 ± 0.2	C1FaeB1	pH 6	7.8 nm	43.3 ± 2.8	19.2 ± 0.6
		8.7 nm	34.3 ± 2.4	15.1 ± 0.6			8.7 nm	53.6 ± 2.7	25.4 ± 2.5
		10.1 nm	<b>39.8 ± 2.3</b>	<b>17.7 ± 0.4</b>			10.1 nm	66.7 ± 1.9	34.9 ± 2.0
		10.2 nm	38.2 ± 1.8	17.5 ± 0.2			10.2 nm	<b>71.7 ± 2.0</b>	<b>37.5 ± 1.0</b>
		MCF	34.1 ± 0.3	12.7 ± 0.0			MCF	50.6 ± 5.8	18.5 ± 3.5
		KIT-6	22.6 ± 2.4	14.3 ± 0.1			KIT-6	41.6 ± 7.7	22.6 ± 6.3
	pH 7	7.8 nm	25.0 ± 1.0	15.0 ± 0.2	pH 7	7.8 nm	45.8 ± 2.6	12.7 ± 4.4	
		8.7 nm	28.9 ± 3.2	15.3 ± 0.7		8.7 nm	46.9 ± 3.5	8.7 ± 3.2	
		10.1 nm	<b>30.0 ± 1.3</b>	<b>15.4 ± 0.5</b>		10.1 nm	46.1 ± 5.3	9.4 ± 3.7	
		10.2 nm	28.7 ± 3.7	15.0 ± 0.7		10.2 nm	<b>54.2 ± 1.7</b>	<b>16.3 ± 1.8</b>	
		MCF	28.5 ± 0.6	14.4 ± 0.2		MCF	45.5 ± 3.4	9.7 ± 3.6	
		KIT-6	21.9 ± 3.2	13.5 ± 0.5		KIT-6	42.5 ± 3.1	11.4 ± 3.1	
C1FaeA2	pH 6	7.8 nm	20.3 ± 2.0	<b>9.1 ± 0.00</b>	C1FaeB2	pH 6	7.8 nm	36.7 ± 7.3	2.6 ± 1.0
		8.7 nm	28.9 ± 4.0	<b>9.1 ± 0.00</b>			8.7 nm	49.6 ± 0.8	<b>2.6 ± 0.2</b>
		10.1 nm	<b>33.7 ± 1.6</b>	<b>9.1 ± 0.00</b>			10.1 nm	54.7 ± 2.5	2.1 ± 0.3
		10.2 nm	31.7 ± 2.2	<b>9.1 ± 0.00</b>			10.2 nm	53.5 ± 8.4	2.4 ± 0.8
		MCF	28.3 ± 3.0	<b>9.1 ± 0.00</b>			MCF	<b>59.6 ± 0.4</b>	2.3 ± 0.2
		KIT-6	14.3 ± 4.0	8.4 ± 0.4			KIT-6	59.5 ± 30.3	n.d.
	pH 7	7.8 nm	19.1 ± 0.4	8.7 ± 0.2	pH 7	7.8 nm	43.5 ± 3.0	1.4 ± 1.3	
		8.7 nm	22.9 ± 2.9	9.2 ± 0.3		8.7 nm	49.7 ± 0.6	2.6 ± 0.6	
		10.1 nm	20.2 ± 4.8	<b>9.4 ± 0.1</b>		10.1 nm	43.7 ± 2.7	1.5 ± 0.5	
		10.2 nm	<b>26.5 ± 4.6</b>	9.3 ± 0.2		10.2 nm	44.0 ± 3.4	1.3 ± 1.3	
		MCF	23.6 ± 0.6	8.7 ± 0.2		MCF	<b>50.3 ± 1.7</b>	<b>3.0 ± 0.5</b>	
		KIT-6	15.0 ± 2.6	7.8 ± 0.2		KIT-6	28.6 ± 4.1	2.0 ± 1.0	

The conditions giving the highest protein or FAE loading are given in boldface.

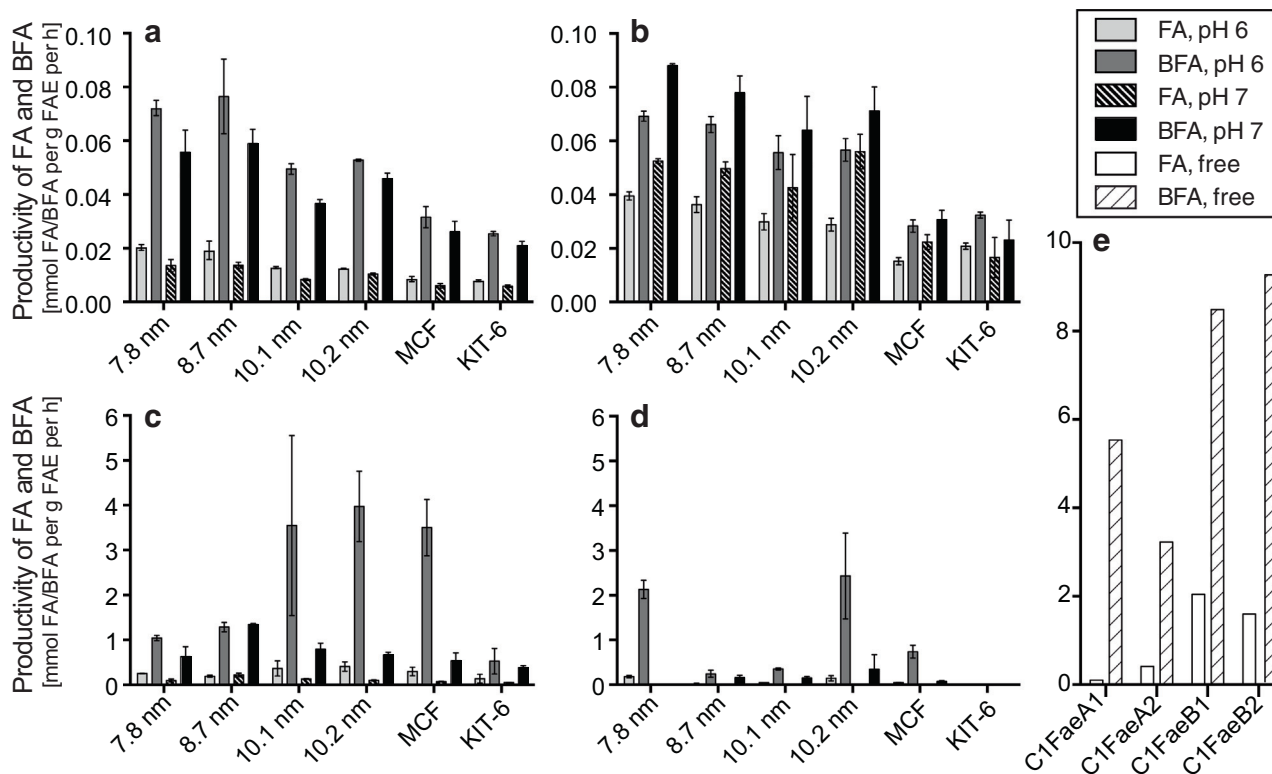


**Fig. 3.** Productivity of BFA and FA. C1FaeA1 (a), C1FaeA2 (b), C1FaeB1 (c) and C1FaeB2 (d) were immobilised at pH 6 or pH 7 on six different MPS substrates, and subsequently subjected to transesterification reactions. Values given are averages of three independent experiments, and error bars indicate the standard deviation. Productivity values of free enzymes are shown in (e). All transesterification reactions were conducted in a 1-butanol-buffer reaction system (92.5:7.5, v/v) at pH 6.5.

the highest values being obtained when using enzymes immobilised at pH 6 on SBA-15 with 7.8 nm pores (2.13 mmol g<sup>-1</sup> h<sup>-1</sup>) and with 10.2 nm pores (2.43 mmol g<sup>-1</sup> h<sup>-1</sup>) (Fig. 3). The large variation in BFA yield when using immobilised C1FaeB2 is probably due to the low amount of FaeB2 enzyme present in the sample, which results in BFA yields close to the detection limit, and thus less robust calculations than in the other three C1 samples.

C1FaeB1 and C1FaeB2 exhibited higher productivities when immobilised at pH 6 than at pH 7 on almost all the support materials, while less pronounced differences were seen in the transesterification efficiencies of C1FaeA1 and C1FaeA2 immobilised at different pHs (Fig. 3). In fact, C1FaeA2 showed better results on five of the six MPS substrates investigated when immobilised at pH 7; the maximum productivity being

0.09 mmol g<sup>-1</sup> h<sup>-1</sup> when immobilised on SBA-15 with 7.8 nm pores. The highest productivities with C1FaeA1 were achieved upon immobilisation on SBA-15 with 7.8 nm pores (0.07 mmol g<sup>-1</sup> h<sup>-1</sup>) and with 8.7 nm pores (0.08 mmol g<sup>-1</sup> h<sup>-1</sup>) at pH 6. In a previous study, it has been shown that native protein structures in aqueous environments are best preserved upon confinement in SBA-15 pores with similar dimensions as the adsorbed proteins (Sang and Coppens, 2011). We observed a similar trend, with the slightly smaller A enzymes (Table 1, Supplementary Fig. S2) having higher transesterification productivities in MPS with smaller pore sizes, while the larger B enzymes showed higher activities in bigger pores. Immobilisation on KIT-6, with pore dimensions close to the theoretical FAE sizes, had detrimental effects on synthetic activities and exhibited the lowest transesterification productivities of all tested supports (Fig. 3). It is possible that on KIT-6, the enzymes were immobilised in a way that restricted the conformational changes necessary for catalysis, or the enzymes might be oriented in such a way that the active site is not accessible for the substrate. Free enzymes showed the best results with productivities 3–14 times higher than their immobilised counterparts (Fig. 3). However, immobilised C1FaeB1 and C1FaeB2 exhibited the highest product selectivity, expressed as the BFA:FA ratio (Fig. 4).

A clear difference in the FA production (i.e., hydrolysis) was observed between the A and B enzymes, as well as between the two immobilised A enzymes. C1FaeA2 produced twice as much FA per gram FAE per hour as C1FaeA1. The stark difference in productivity and selectivity between the A and B type enzymes could be attributed to structural differences between the two, especially in the area around the catalytic site. Alignment of homology models of the proteins revealed that the type A and B FAEs of *M. thermophila* have a similar overall architecture with an  $\alpha/\beta$ -hydrolase fold. However, FaeB1 and FaeB2 have three unique loops to the left of the active site, including three  $\alpha$ -helices, while FaeA1 and FaeA2 have three unique loops to the right of the active site (Supplementary Fig. S8). A higher amount of hydrophobic amino acids around the catalytic centre could influence the preference for transesterification over hydrolysis, however, the A and B type enzymes appeared to have very similar hydrophobicity around the active site. Four cysteine residues are present in FaeB1 and FaeB2, close to the putative catalytic residues aspartic acid and serine (Topakas et al., 2012), which could form disulphide bridges (Supplementary Fig. S9). The increased rigidity, and thus more stable conformation, introduced by disulphide bridges could contribute to both the higher productivity and higher BFA:FA ratios of the B enzymes.

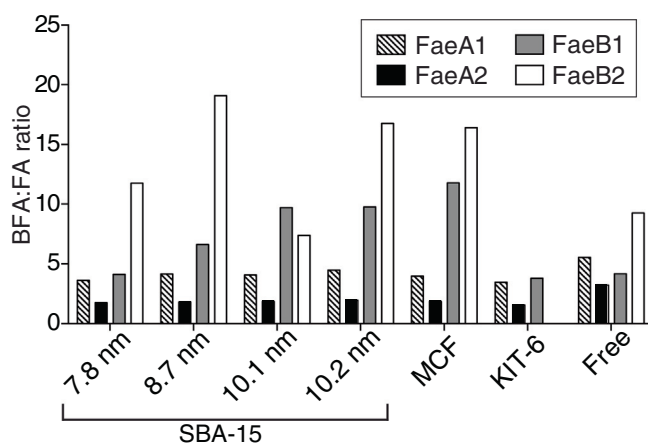


Fig. 4. BFA:FA ratio in the transesterification reaction using enzymes immobilised on the six MPS substrates at pH 6, as well as for free enzymes.

Similarly, the higher selectivity exhibited by immobilised FaeB1 and FaeB2, compared to their free counterparts, could also be due to changes in enzyme structure resulting from adsorption onto the support material. The lack of a beneficial effect of immobilisation on the selectivity of FaeA1 and FaeA2 indicates that rather than being a general effect of immobilisation, it seems to be enzyme (structure)-dependent. This however needs to be investigated further.

#### 3.4. Effect of solvent rinsing on transesterification yield

The yield and reaction rate of enzyme reactions in organic solvents are influenced by the water content in the system (Herbst et al., 2012; Zaks and Klibanov, 1988). To maintain a low water concentration, immobilised enzymes are usually dried under vacuum before addition to the reaction medium. An alternative way to remove water is successive rinsing of immobilised enzymes with an organic solvent, a method that was originally performed with propanol (Partridge et al., 1998) and thus called propanol-rinsed enzyme preparation (PREP). It has been suggested to lead to better retention of protein conformation, higher activity and improved transacetylation yields, compared to freeze-dried preparations (Majumder et al., 2007).

PREPs of C1FaeB1, immobilised on SBA-15 with 10.2 nm pores, were prepared with three different organic solvents: ethanol, propanol and 1-butanol. Water content was adjusted to match the final water activity ( $a_w$ ) in our reaction system (7.5% in 1-butanol,  $a_w$  0.234). In addition, PREPs with propanol with  $a_w = 0$  (no water) and with  $a_w = 0.2$  (corresponding to 7.5% water in 1-propanol) were also investigated. All solvent-rinsed enzyme preparations of C1FaeB1 performed better in the subsequent transesterification reactions than the vacuum-dried preparations with all but one of the PREPs showing twice the productivity of the dried enzyme preparations (Fig. 5a). Solvent rinsing with 1-propanol,  $a_w = 0$ , resulted in a similar productivity to drying. The different solvents, as well as small differences in water activity (0.2 vs. 0.243) had only minor effects on the BFA production rate. The use of PREPs increased the productivity of the immobilised enzymes so that the values approached those of the free enzyme sample, whose productivity was about 1.2 times that of the 1-butanol PREP (Fig. 5a).

The storage of immobilised enzymes at 4 °C, either dried or in the solvents used for solvent rinsing, was also evaluated (Fig. 5b). All preparations were stable over the course of 23 days. The lower overall performance and slight decrease in storage stability of dried immobilised enzymes and PREP 1-propanol,  $a_w = 0$ , may be due to irreversible conformational changes in the proteins in the absence of water during the dehydration step.

#### 3.5. Reuse of immobilised enzymes

Reusability is one of the most important advantages of immobilised enzymes over free enzymes, and can lead to a substantial reduction in the production cost. The dried and solvent-rinsed preparations of immobilised enzymes (FaeB1 on SBA-15 with 10.2 nm pores) were tested over 9 reaction cycles, each one lasting 24 h. The immobilised enzymes showed excellent stability, with both BFA production rate and selectivity (BFA:FA ratio) being almost constant over the nine cycles (Fig. 5c–e). At the end of cycle 9, the productivity had decreased by only 8%, at most, compared to cycle 1 (Fig. 5d). BFA productivity and BFA:FA ratio of one time point of free enzymes are included in Fig. 5c,e for comparison. Reactions with free enzyme resulted in by far the lowest BFA:FA ratio (4.2), followed by dried immobilised enzyme preparation (6.5). The best selectivity was achieved with PREPs 1-propanol,  $a_w = 0$ , giving a value of 15.5. Thus, the best solvent-rinsed enzyme preparation resulted in an almost four times better

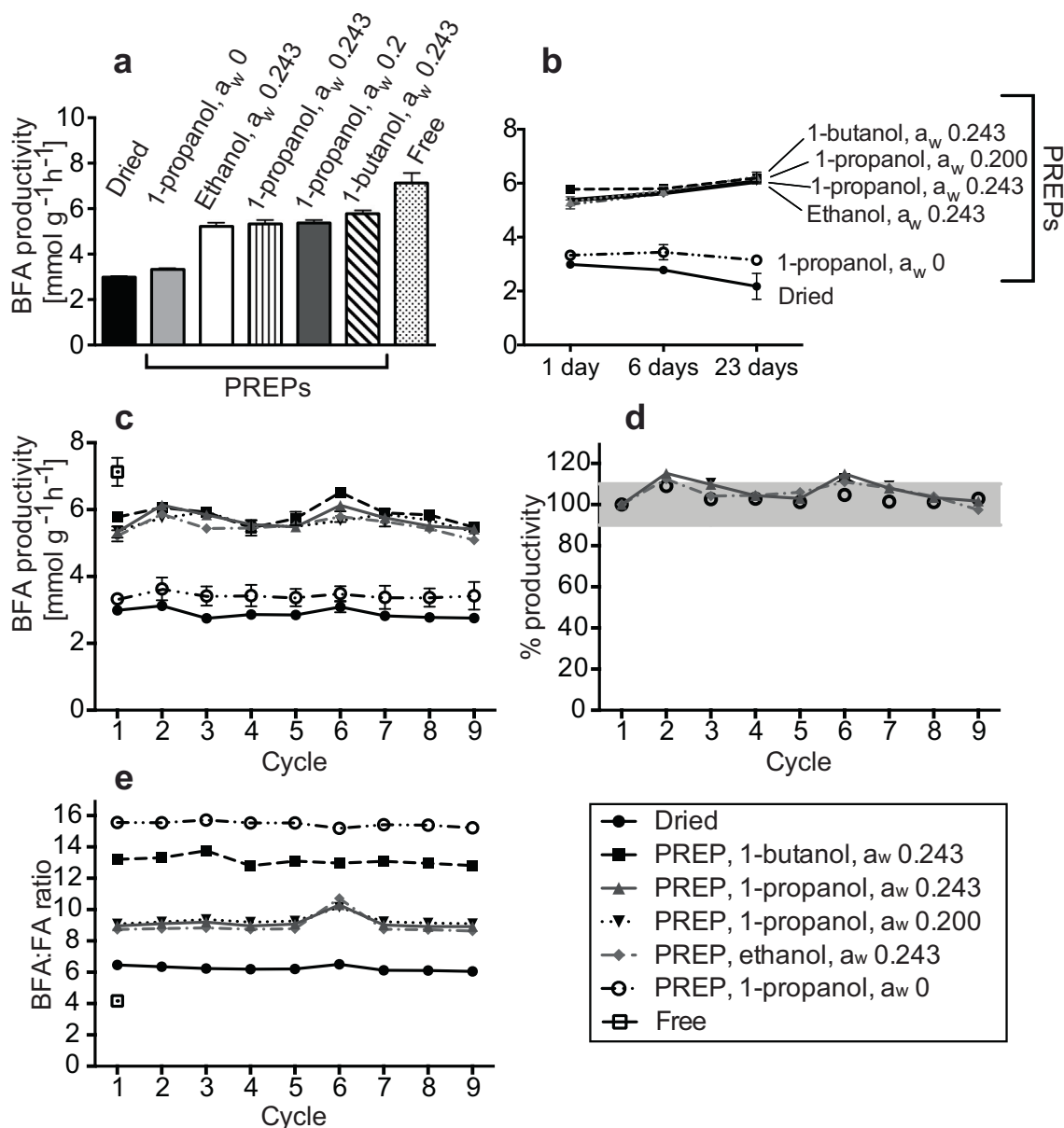


**Fig. 5.** Productivity of BFA, storage stability and reusability of immobilised enzymes. Enzymes from sample C1FaeB1 immobilised on SBA-15 with pore size 10.2 nm were either dried after immobilisation or solvent-rinsed (PREPs) with 1-butanol, 1-propanol or ethanol with varying water activities ( $a_w$ ), before being used in transesterification reactions to yield BFA. Free enzyme was used in buffer. (a) BFA productivity of freshly prepared immobilised enzyme. (b) Immobilised enzymes that had been stored in the respective solvent, or dried, at 4 °C for the indicated number of days before being used in transesterification reactions. (c–e) Reusability of immobilised enzymes: (c) Productivity of BFA over 9 reaction cycles. (d) Productivity in percent, in relation to cycle 1 (= 100%). The shaded area indicates 90–110%. (e) BFA:FA ratio over 9 reaction cycles. Values are averages of three independent experiments, and error bars indicate the standard deviation.

synthesis-to-hydrolysis ratio than free enzyme. The complete absence of water in the 1-propanol PREP,  $a_w = 0$  might induce a conformational change in the protein structure that shields the active site of the enzyme from water in the later reaction, favouring transesterification over hydrolysis. The fact that this effect is not present in the dried enzyme preparation indicates that it is caused by the solvent rather than simply dehydration.

#### 4. Conclusions

Immobilisation of FAEs on MPS resulted in stable biocatalysts that could be reused for several production cycles without significant loss of activity. Enrichment of the target enzyme, compared to other proteins in the crude culture filtrate, could be achieved on the support material by carefully choosing the pore size of the

MPS. Product selectivity for the two type B FAEs could be greatly improved by adsorption onto MPS. Solvent rinsing further improved both productivity and selectivity of immobilised enzymes.

#### Acknowledgements

This work was supported by the European Union OPTIBIOCAT Project (FP7 KBBE. 2013.3.3-04; Grant Agreement No. 613868). The authors have no conflict of interest to declare.

#### Appendix A. Supplementary data

Supplementary data associated with this article can be found, in the online version, at <http://dx.doi.org/10.1016/j.biortech.2017.04.106>.

## References

- Antonopoulou, I., Varriale, S., Topakas, E., Rova, U., Christakopoulos, P., Faraco, V., 2016. Enzymatic synthesis of bioactive compounds with high potential for cosmeceutical application. *Appl. Microbiol. Biotechnol.* 100, 6519–6543.
- Barone, E., Calabrese, V., Mancuso, C., 2009. Ferulic acid and its therapeutic potential as a hormetin for age-related diseases. *Biogerontology* 10, 97–108.
- Barrett, E.P., Joyner, L.G., Halenda, P.P., 1951. The determination of pore volume and area distributions in porous substances. 1. Computations from nitrogen isotherms. *J. Am. Chem. Soc.* 73 (1), 373–380.
- Brady, D., Jordaán, J., 2009. Advances in enzyme immobilisation. *Biotechnol. Lett.* 31, 1639–1650.
- Brunauer, S., Emmett, P.H., Teller, E., 1938. Adsorption of gases in multimolecular layers. *J. Am. Chem. Soc.* 60, 309–319.
- Cao, L., 2005. Immobilised enzymes: science or art? *Curr. Opin. Chem. Biol.* 9, 217–226.
- Carrea, G., Riva, S., 2000. Properties and synthetic applications of enzymes in organic solvents. *Angew. Chem. Int. Ed. Engl.* 39, 2226–2254.
- Chouyyok, W., Panpranot, J., Thanachayanant, C., Prichanont, S., 2009. Effects of pH and pore characters of mesoporous silicas on horseradish peroxidase immobilization. *J. Mol. Catal. B: Enzym.* 56, 246–252.
- Crepin, V.F., Faulds, C.B., Connerton, I.F., 2004. Functional classification of the microbial feruloyl esterases. *Appl. Microbiol. Biotechnol.* 63, 647–652.
- Dunker, A.K., Fernández, A., 2007. Engineering productive enzyme confinement. *Trends Biotechnol.* 25, 189–190.
- Eş, I., Vieira, J.D.G., Amaral, A.C., 2015. Principles, techniques, and applications of biocatalyst immobilization for industrial application. *Appl. Microbiol. Biotechnol.* 99, 2065–2082.
- Essa, H., Magner, E., Cooney, J., Hodnett, B.K., 2007. Influence of pH and ionic strength on the adsorption, leaching and activity of myoglobin immobilized onto ordered mesoporous silicates. *J. Mol. Catal. B Enzym.* 49, 61–68.
- Faulds, C.B., 2010. What can feruloyl esterases do for us? *Phytochem. Rev.* 9, 121–132.
- Giuliani, S., Piana, C., Setti, L., Hochkoepller, A., Pifferi, P.G., Williamson, G., Faulds, C.B., 2001. Synthesis of pentyferulate by a feruloyl esterase from *Aspergillus niger* using water-in-oil microemulsions. *Biotechnol. Lett.* 23, 325–330.
- Gopalan, N., Rodríguez-Duran, L.V., Saucedo-Castaneda, G., Nampoohiri, K.M., 2015. Review on technological and scientific aspects of feruloyl esterases: a versatile enzyme for biorefining of biomass. *Bioresour. Technol.* 193, 534–544.
- Gustafsson, H., Johansson, E.M., Barrabino, A., Odén, M., Holmberg, K., 2012. Immobilization of lipase from *Mucor miehei* and *Rhizopus oryzae* into mesoporous silica—the effect of varied particle size and morphology. *Colloids Surfaces B Biointerfaces* 100, 22–30.
- Herbst, D., Peper, S., Niemeyer, B., 2012. Enzyme catalysis in organic solvents: influence of water content, solvent composition and temperature on *Candida rugosa* lipase catalyzed transesterification. *J. Biotechnol.* 162, 398–403.
- Hudson, E.P., Eppler, R.K., Clark, D.S., 2005. Biocatalysis in semi-aqueous and nearly anhydrous conditions. *Curr. Opin. Biotechnol.* 16, 637–643.
- Kelly, L.A., Mezulis, S., Yates, C., Wass, M., Sternberg, M., 2015. The Phyre2 web portal for protein modelling, prediction, and analysis. *Nat. Protoc.* 10, 845–858.
- Kikuzaki, H., Hisamoto, M., Hirose, K., Akiyama, K., Taniguchi, H., 2002. Antioxidant properties of ferulic acid and its related compounds. *J. Agric. Food. Chem.* 50, 2161–2168.
- Kleitz, F., Choi, S.H., Ryoo, R., 2003. Cubic Ia3d large mesoporous silica: synthesis and replication to platinum nanowires, carbon nanorods and carbon nanotubes. *Chem. Commun. (Camb)*, 2136–2137.
- Krieger, E., Vriend, G., 2014. YASARA View – molecular graphics for all devices – from smartphones to workstations. *Bioinformatics* 30, 2981–2982.
- Kroon, P.A., Garcia-cones, M.T., Fillingham, I.J., Hazlewood, G.P., Williams, G., 1999. Release of ferulic acid dehydrodimers from plant cell walls by feruloyl esterases. *J. Sci. Food Agric.* 79, 428–434.
- Kühnel, S., Pouvreau, L., Appeldoorn, M.M., Hinz, S.W.A., Schols, H.A., Gruppen, H., 2012. The ferulic acid esterases of *Chrysosporium lucknowense* C1: purification, characterization and their potential application in biorefinery. *Enzyme Microb. Technol.* 50, 77–85.
- Lei, C., Shin, Y., Liu, J., Ackerman, E.J., 2007. Synergetic effects of nanoporous support and urea on enzyme activity. *Nano Lett.* 7, 1050–1053.
- Lukens, W.W., Schmidt-Winkel, P., Zhao, D., Feng, J., Stucky, G.D., 1999. Evaluating pore sizes in mesoporous materials: a simplified standard adsorption method and a simplified Broekhoff-de Boer method. *Langmuir* 15, 5403–5409.
- Magner, E., 2013. Immobilisation of enzymes on mesoporous silicate materials. *Chem. Soc. Rev.* 42, 6213–6222.
- Majumder, A.B., Shah, S., Gupta, M.N., 2007. Enantioselective transacetylation of (R, S)-beta-citronellol by propanol rinsed immobilized *Rhizomucor miehei* lipase. *Chem. Cent. J.* 1, 10.
- Matsuo, T., Kobayashi, T., Kimura, Y., Tsuchiyama, M., Oh, T., Sakamoto, T., Adachi, S., 2008. Synthesis of glyceryl ferulate by immobilized ferulic acid esterase. *Biotechnol. Lett.* 30, 2151–2156.
- Moelans, D., Cool, P., Baeyens, J., Vansant, E.F., 2005. Immobilisation behaviour of biomolecules in mesoporous silica materials. *Catal. Commun.* 6, 591–595.
- Partridge, J., Halling, P.J., Moore, B.D., 1998. Practical route to high activity enzyme preparations for synthesis in organic media. *Chem. Commun.*, 841–842.
- Sang, L.-C., Coppens, M.-O., 2011. Effects of surface curvature and surface chemistry on the structure and activity of proteins adsorbed in nanopores. *Phys. Chem. Chem. Phys.* 13, 6689–6698.
- Schmidt-Winkel, P., Lukens, W.W., Yang, P., Margolese, D.I., Lettow, J.S., Ying, J.Y., Stucky, G.D., 2000. Microemulsion templating of siliceous mesostructured cellular foams with well-defined ultralarge mesopores. *Chem. Mater.* 12, 686–696.
- Serdakowski, A.L., Dordick, J.S., 2008. Enzyme activation for organic solvents made easy. *Trends Biotechnol.* 26, 48–54.
- Sheldon, R.A., van Pelt, S., 2013. Enzyme immobilisation in biocatalysis: why, what and how. *Chem. Soc. Rev.* 42, 6223–6235.
- Singh, R.K., Tiwari, M.K., Singh, R., Lee, J.K., 2013. From protein engineering to immobilization: promising strategies for the upgrade of industrial enzymes. *Int. J. Mol. Sci.* 14, 1232–1277.
- Soares, C.M., Teixeira, V.H., Baptista, A.M., 2003. Protein structure and dynamics in nonaqueous solvents: insights from molecular dynamics simulation studies. *Biophys. J.* 84, 1628–1641.
- Stepankova, V., Bidmanova, S., Koudelakova, T., Prokop, Z., Chaloupkova, R., Damborsky, J., 2013. Strategies for stabilization of enzymes in organic solvents. *ACS Catal.* 3, 2823–2836.
- Tan, Z., Shahidi, F., 2011. Chemoenzymatic synthesis of phytosteryl ferulates and evaluation of their antioxidant activity. *J. Agric. Food Chem.* 59, 12375–12383.
- Tawat, S., Taira, S., Kobamoto, N., Zhu, J., Ishihara, M., Toyama, S., 1996. Synthesis and antifungal activity of cinnamic acid esters. *Biosci. Biotechnol. Biochem.* 60, 909–910.
- Thörn, C., Gustafsson, H., Olsson, L., 2011. Immobilization of feruloyl esterases in mesoporous materials leads to improved transesterification yield. *J. Mol. Catal. B Enzym.* 72, 57–64.
- Thörn, C., Udatha, D.B.R.K.G., Zhou, H., Christakopoulos, P., Topakas, E., Olsson, L., 2013. Understanding the pH-dependent immobilization efficacy of feruloyl esterase-C on mesoporous silica and its structure–activity changes. *J. Mol. Catal. B Enzym.* 93, 65–72.
- Topakas, E., Moukoulis, M., Dimarogona, M., Christakopoulos, P., 2012. Expression, characterization and structural modelling of a feruloyl esterase from the thermophilic fungus *Myceliophthora thermophila*. *Appl. Microbiol. Biotechnol.* 94, 399–411.
- Vafiadi, C., Topakas, E., Nahmias, V.R., Faulds, C.B., Christakopoulos, P., 2009. Feruloyl esterase-catalysed synthesis of glycerol sinapate using ionic liquids mixtures. *J. Biotechnol.* 139, 124–129.
- Visser, H., Joosten, V., Punt, P.J., Gusakov, A.V., Olson, P.T., Joosten, R., Bartels, J., Visser, J., Sinitsyn, A.P., Emalfarb, M.A., Verdoes, J.C., Wery, J., 2011. Development of a mature fungal technology and production platform for industrial enzymes based on a *Myceliophthora thermophila* isolate, previously known as *Chrysosporium lucknowense* C1. *Ind. Biotechnol.* 7, 214–224.
- Vulfson, E.N., Halling, P.J., 2001. Enzymes in Nonaqueous Solvents: Methods and Protocols. Springer Science & Business Media. vol. 15.
- Yang, L., Dordick, J.S., Garde, S., 2004. Hydration of enzyme in nonaqueous media is consistent with solvent dependence of its activity. *Biophys. J.* 87, 812–821.
- Yue, Q., Yang, H.J., Li, D.H., Wang, J.Q., 2009. A comparison of HPLC and spectrophotometrical methods to determine the activity of ferulic acid esterase in commercial enzyme products and rumen contents of steers. *Anim. Feed Sci. Technol.* 153, 169–177.
- Zaks, A., Klibanov, A.M., 1988. The effect of water on enzyme action in organic media. *J. Biol. Chem.* 263, 8017–8021.
- Zhou, Z., Hartmann, M., 2012. Recent progress in biocatalysis with enzymes immobilized on mesoporous hosts. *Top. Catal.* 55, 1081–1100.